Published in final edited form as:
Ann Neurol. 2010 November ; 68(5): 703–716. doi:10.1002/ana.22090.

Oligodendrocyte *PTEN* required for myelin and axonal integrity not remyelination

Emily P. Harrington, BA[1,2], **Chao Zhao, PhD**[3], **Stephen P.J. Fancy, DVM, PhD**[1], **Sovann Kaing, BS**[1], **Robin J.M. Franklin, PhD**[3], and **David H. Rowitch, MD, PhD**[1,#]

[1] Departments of Pediatrics and Neurosurgery, Eli and Edyth Broad Institute for Stem Cell Research and Regeneration Medicine and Howard Hughes Medical Institute, San Francisco, CA, 94143, USA

[2] Medical Scientist Training Program, University of California San Francisco, 513 Parnassus Avenue, San Francisco, CA, 94143, USA

[3] MRC Centre for Stem Cell Biology and Regenerative Medicine and Department of Veterinary Medicine, University of Cambridge, Madingley Road, Cambridge CB3 0ES, UK

Abstract

Objective—Repair of myelin injury in multiple sclerosis may fail resulting in chronic demyelination, axonal loss and disease progression. As cellular pathways regulated by *Phosphatase and tensin homologue deleted on chromosome 10 (PTEN;* e.g., PI-3Kinase) have been reported to enhance axon regeneration and oligodendrocyte maturation, we investigated potentially beneficial effects of *Pten* loss-of-function in the oligodendrocyte lineage on remyelination.

Methods—We characterized oligodendrocyte numbers and myelin sheath thickness in mice with conditional inactivation of PTEN in oligodendrocytes, *Olig2-cre, Pten*$^{fl/fl}$ mice. Utilizing a model of CNS demyelination, lysolecithin injection into the spinal cord white matter, we performed short and long-term lesioning experiments and quantified oligodendrocyte maturation and myelin sheath thickness in remyelinating lesions.

Results—During development, we observed dramatic hypermyelination in the corpus callosum and spinal cord. Following white matter injury, however, there was no detectable improvement in myelin repair. Moreover, we observed progressive myelin sheath abnormalities and massive axon degeneration in the fasciculus gracilis of mutant animals, as indicated by ultrastructure and expression of SMI-32, APP and Caspase 6.

Interpretation—These studies indicate adverse effects of chronic *PTEN* inactivation (and by extension, activation PI-3K signaling) on myelinating oligodendrocytes and their axonal targets. We conclude that *Pten* function in oliogodendrocytes is required to regulate myelin thickness and preserve axon integrity. In contrast, *Pten* is dispensable during myelin repair and its inactivation confers not detectable benefit.

Introduction

Rapid saltatory conduction of action potentials in the central nervous system (CNS) depends on myelination. Oligodendrocytes perform this role by wrapping axons with multilaminar extensions of plasma membrane. Demyelination, the loss of myelin sheaths around axons, can result in impaired conduction of neuronal impulses and prolonged failure to remyelinate

[#]Author for correspondence: D.H. Rowitch (rowitchd@peds.ucsf.edu).

axons can result in axonal degeneration and neuronal cell death[1]. Clinically significant demyelinating disorders can be caused by (1) intrinsic defects in oligodendrocyte lineage cells themselves (e.g., leukodystrophies), (2) damage to developing oligodendrocytes in the preterm neonate (e.g., periventricular leukomalacia)[2], (3) T lymphocyte depletion and resulting toxic leukoencephalopathy, a side effect of certain immune modulatory monoclonal antibodies[3] and (4) inflammatory/autoimmune-mediated damage to myelin and oligodendrocytes, as occurs in multiple sclerosis (MS).

Remyelination in MS lesions is often variable: in some lesions remyelination is extensive, while in other lesions remyelination is incomplete or absent. Remyelination is extensive in a subset of multiple sclerosis patients[4] in which it restores conduction to demyelinated axons[5] and may protect axons from degeneration[6]. In MS patients, clinical disability has been shown to correlate with axonal damage[7] and resulting axon loss is thought to be a major contributor to neurological disability[8]. Remyelination efficiency also declines with age[9,10] and aging is associated with more severe axonal degeneration after demyelination[11].

Following demyelination oligodendrocyte progenitor cells (OLPs) (1) respond to inflammatory cues and (2) migrate to the injured area where they (3) proliferate and (4) undergo differentiation into mature oligodendrocytes capable of remyelination. Remyelination failure in the complex setting of the MS plaque can be caused by factors that impair or alter the kinetics of any/all of the above-mentioned steps (1–4), the final step of differentiation and myelination seemingly the most vulnerable to dysregulation[12]. Indeed, a characteristic of remyelinated axons in MS and experimental rodent systems is that the thickness of the myelin sheathes is significantly reduced compared with undamaged white matter. In MS, such areas are called “shadow plaques” on account of their reduced myelin staining intensity compared to normal, undamaged white matter.

Phosphatase and tensin homologue deleted on chromosome 10 (PTEN) encodes a lipid phosphatase that antagonizes the phosphatidylinositol-3-kinase (PI-3K) signaling pathway by converting phosphatidylinositol 3,4,5-trisphosphate (PIP_3) into phosphatidylinositol 4,5-bisphosphate (PIP_2) (Fig 1A). Deletion of *PTEN* results in over-activation of the Akt and downstream Akt targets such as mammalian target of rapamycin (mTOR), which plays a critical role in the regulation of cell growth, mRNA translation, and ribosomal biogenesis. In humans, *PTEN* deletion is characteristic of many high-grade glial tumors.

Recent reports have demonstrated involvement of the PI-3K pathway in CNS myelination and OLP differentiation. Transgenic mice with forced expression of activated Akt in oligodendrocytes develop dramatic hypermyelination[13] and increased myelin thickness through an mTOR-dependent mechanism[14]. mTOR activation has also been demonstrated to promote OLP differentiation[15]. These findings suggest a potential therapeutic benefit to activation of the PI-3K/mTOR pathway to enhance remyelination.

To test this and a potential novel requirement for *PTEN* during oligodendrocyte development and repair, we generated *Olig2-cre, Pten*$^{fl/fl}$ mice in which conditional deletion of *PTEN* occurs in all oligodendrocytes and their precursors. Our data demonstrate an essential role for *PTEN* function in the regulation of myelin sheath thickness and myelin and axon integrity. During remyelination however, we found no benefit to *PTEN* deletion in oligodendrocytes.

Materials and Methods

Animals

All animal procedures were conducted in complete compliance with the National Institute of Health *Guide for the Care and Use of Laboratory* Animals and were approved by the Institutional Animal Care and Use Committee at the University of California, San Francisco. *Olig2-tva-Cre* mice were generated by insertion of a TVA receptor and IRES-Cre cassette into the endogenous Olig2 locus as previously described[16] allowing for Cre mediated recombination in oligodendrocyte lineage cells. *Olig2-tva-Cre*$^{+/-}$ mice were crossed for two generations onto *Pten*$^{fl/fl}$ mice (gift from Ronald A. DePinho), to generate *Olig2-tva-cre*+/− *Pten*$^{fl/fl}$ mice that were maintained on a C57BL/6 background. For fate mapping experiments *Olig2-tva-cre*+/− *Pten*$^{fl/fl}$ mice were crossed to conditional reporter *ROSA26-YFP*$^{fl/fl}$ (*Gt(ROSA)26*$^{Sortml(EYFP)Cos}$*/J*, Jackson laboratory Bar Harbour, ME) mice and maintained on a C57BL/6 background.

Demyelination with lysolecithin injection

Olig2-cre, Pten$^{fl/fl}$ and *Pten*$^{fl/fl}$ littermates 8–12 weeks-old were used for lyolecithin demyelinating studies. Anesthesia was induced with inhaled isoflurane/oxygen, supplemented with 0.05ml buprenorphine (0.05mg/ml). Dorsal laminectomy was performed at the T12/T13 level, a Hamilton needle was advanced lateral to the central vein at a 45° angle, and 0.5μl of 1% lysolecithin (Lα-lysophosphatidylcholine, Sigma) was injected into the ventrolateral white matter.

Oligodendrocyte progenitor cultures

OPCs were isolated by immunopanning postnatal day 7 *Olig2-cre, Pten*$^{fl/fl}$ and *Pten*$^{fl/fl}$ mouse cerebral cortices. *Olig2-cre, Pten*$^{fl/fl}$ and *Pten*$^{fl/fl}$ P7 littermates were euthanized and decapitated. Cerebral hemispheres were dissected out and dissociated by incubation in papain (Worthington) for 90 minutes at 34°C in 5% CO_2 95% O_2. After dissociation ovomucoid (Worthington) was used to quench enzymatic activity. Cells were resuspended in panning buffer (0.02% BSA, 5ng/ml insulin in D-PBS) passed through 20μm filter and added to pre-coated BSL1 dish. BSL1 dish was prepared by incubation of BSL1 1:1000 (Vector L-1100) in D-PBS overnight at 4°C. Cells were incubated on BSL1 dish for 1 hour at room temperature. Non-adherent cell suspension was transferred to a PDGFRα dish that was prepared by adding goat anti-rat IgG (H+L) 1:333 (Jackson 112-005-003) in 50mM Tris pH 9.5 overnight at 4°C followed by incubation with rat anti-PDGFRα 1:300 (BD Pharmigen 558774) in 0.2% BSA for 3 hours at room temperature. Cells suspension was incubated on PDGFRα dish for 3 hours at room temperature. Non-adherent cell suspension was discarded and plate was rinsed with D-PBS to remove non-adherent cells. Adherent OPCs were collected by brief trypsinzation and resuspended in proliferation media. OPCs were plated on poly-D-lysine coated coverslips and maintained in proliferation media in a 10% CO_2 37°C incubator. Proliferation media: 2mM glutamine, 5ng/ml N-acetyl-L-cysteine, 1mM sodium pyruvate, 1x Pen/Strep, 1x Trace Elements B (Cellgro), 10ng/ml d-Biotin, 5ng/ml insulin, B27 without T3, 5nM Forskolin, 1x SATO (100μg/ml transferrin, 100μg/ml BSA, 10μg/ml putrescine, 60ng/ml progesterone, 40ng/ml sodium selenite), 10ng/ml CNTF (Peprotech), 10ng/ml PDGF-AA (Peprotech), 1ng/ml NT-3 (Peprotech) in high glucose DMEM (Gibco 11960). After 12 hours coverslips were fixed with 4% paraformaldehyde in DMEM for 10 minutes followed by two washes in PBS.

Immunohistochemistry

Mice were deeply anesthetized with isoflurane and perfused transcardially with phosphate buffered saline (PBS) followed by 4% paraformaldehyde in PBS. After dissection tissue

samples were fixed in 4% paraformaldehyde in PBS overnight at 4°C, equilibrated in 20% sucrose v/w for 1 day, embedded in OCT (Tissue-Tek), frozen on dry ice and stored at −80°C. 14μm tissue sections were cut on a Leica cryostat and mounted onto slides. Slides were rinsed with PBS, and antigen retrieval was performed by incubating slides for 10 minutes in 10mM sodium citrate pH 6 at 95°C. For DAB staining, slides were incubated in 1% H_2O_2 for 10 minutes. Slides were incubated for 1 hour at room temperature in blocking solution 5% normal goat serum 0.1% TritonX-100 in PBS (PBST). Primary antibody was added in blocking solution and incubated overnight at 4°C. Primary antibodies: Olig2 1:20,000 (generous gift from CD Stiles, Harvard), Nkx2.2 1:100 (DSHB 74.5A5), APC 1:500 (Calbiochem OP80), Ki67 1:000 (Novocastra NCL-Ki67p), SMI-32 1:1000 (Covance SMI-32R), Caspase-6 1:50 (BD Pharmigen 556581), APP 1:100 (Millipore MAB348), Caspr 1:500 (Abcam ab34151), pan-sodium channel (Sigma S8809), CD45 1:00 (Millipore CBL1326), CD3 (Dako A0452), Iba1 1:500 (Wako 019-19741), Phospho-S6 1:100 (Cell Signaling 2211), Pten 1:100 (Cell Signaling 9559), GFP 1:500 (Millipore 06-896), Cleaved caspase-3 1:500 (Cell Signaling 9661S). For Nkx2.2 and APC staining on lesion sections M.O.M. blocking reagents (Vector) were used to reduce non-specific background. After primary incubation slides were washed in PBST 3×10 minutes.

Slides were incubated in biotinylated secondary antibodies (Vector) or Alexa Fluor secondary antibodies (Molecular Probes) 1:500 in blocking solution for 1 hour at room temperature. Slides were washed 3×10 minutes in PBST. Immunofluorescent slides were incubated in DAPI (Calbiochem) 1μg/ml for 5 minutes and coversliped in Fluoromount-G (SouthernBiotech). DAB sections were incubated in ABC solution (Vector) for 90 minutes at room temperature, washed 3×10 in PBST, and developed in 0.5mg/ml DAB+0.01% H_2O_2 in PBS for 1–5 minutes. Slides were then dehydrated in ascending ethanol concentrations followed by xylene and mounting with Permount (Fisher).

In situ Hybridization

PLP/DM20 probe was prepared and diluted in hybridization buffer, as previously described[17] denatured for 10 minutes at 75°C, and added directly to air-dried slides. Slides were coversliped, placed in an incubation chamber with 50% formamide and 1X SSC in DEPC treated dH_2O, and hybridized overnight at 65°C. After hybridization slides were incubated in wash buffer (1X SSC, 50% formamide, 0.1% Tween-20) at 65°C for 15 minutes. Slides were washed in wash buffer 2×30 minutes at 65°C and washed 2×10 minutes in MABT (100mM maleic acid, 150mM NaCl, 0.1%Tween-20 pH 7.5) at room temperature. Slides were then incubated in blocking solution (2% blocking reagent (Boehringer) and 10% heat-inactivated sheep serum in MABT) for one hour at room temperature. Anti-digoxygenin-AP fragments (Roche) 1:1500 in blocking solution was added to slides and slides were incubated overnight at 4°C. After overnight incubation slides were washed 3×10 minutes in MABT, 2×10 minutes in staining buffer (100mM Tris-HCl, 100mM NaCl, 5mM $MgCl_2$ pH 9) followed by incubation in BCIP/NBT stock solution (Roche) at 37°C for 1–2 hours. Slides were coversliped with Aquamount (ThermoScientific).

Western Blot

Mice were anesthetized with isoflurane and tissue was dissected out, immediately flash frozen on dry ice and stored at −80°C. Tissue lysed in cold RIPA buffer (ThermoScientific) with protease inhibitor cocktail (Sigma P8340), phosphate inhibitor (Calbiochem 524629) and 5mM EDTA. Samples were homogenized by passage through a large bore needle then incubated on ice for 15 minutes, centrifuged at 14,000rpm for 15 minutes at 4°C. Supernantant was collected and protein concentration measured using protein assay reagent (Biorad). Samples were stored at −80°C or used immediately for western blotting. Samples

were diluted in Laemmli buffer with 1mM DTT and heated at 95°C for 5 minutes. 40μg protein/well was loaded in SDS-PAGE gel and run in running buffer (25mM Tris base, 190mM glycine, 0.1% SDS) at 90V for 2 hours. Gels were transferred to PVDF membranes in transfer buffer (25mM Tris base, 190mM glycine, 20% methanol) at 350mA for 1 hour at 4°C. Blots were blocked in 5% milk or 5% BSA in TBST (1XTBS+0.1% Tween-20) for 1 hour followed by incubating in primary antibody in blocking solution overnight at 4°C. Primary antibodies: Phospho-p70 S6K Thr389 1:1000 (Cell Signaling 9205) Phospho-Akt Ser473 1:1000 (Cell Signaling 4060), Akt 1:1000 (Cell Signaling 4691), Pten 1:1000 (Cell Signaling 9559), β-tubulin 1:10,000 (Millipore MAB3408). After primary incubation membranes were washed 3×10 minutes in TBST and incubated in HRP-conjugated secondary antibody (ThermoScientific) 1:10,000 in TBST for 1 hour at room temperature. Membranes were washed again 3×10 minutes in TBST and incubated in ECL Plus reagent (Amersham) and developed on Kodak BioMax film.

Electron Microscopy

Mice were deeply anesthetized and perfused transcardially with PBS followed by 4% glutaraldehyde 0.008% $CaCl_2$ in PBS. Tissue was post-fixed in glutaraldehyde solution then cut transversely into 1.0mm-thick blocks. Blocks were further fixed in osmium tetroxide at 4 C overnight, dehydrated through ascending ethanol washes, and embedded in TAAB resin (TAAB Laboratories, Aldermaston, UK). 1μm sections were cut, stained with toluidine blue, and examined by light microscopy, from which remyelination was identified using standard morphological criteria. Remyelinating lesion blocks were examined by electron microscopy (Hitachi, H600). G-ratio calculations of axons in the area of interest were calculated by dividing the diameter of an axon by the diameter of axon plus the associated myelin sheath. Approximately 100–200 axons each group of 3–4 animals were used. Briefly, images of transverse sections in lesioned white matter of the ventral column of the spinal cord were taken at 6000x magnification; corpus callosum was sampled above the lateral ventricles and transverse images were taken at 10,000x magnification Digitized and calibrated images were analyzed using ImageJ (NIH). Linear regression was used for indicating the differences between two groups in myelin thickness across the range of axon diameters, by comparing the slope and interception on Y axis. Overall g-ratio was compared by unpaired t test using Graphpad Prism. Statistical significance was set at $p<0.05$.

Quantification and Statistics

Microscopy was performed on a Zeiss AxioScope 2 and images were taken with AxioCam camera. Cell counts images were analyzed in ImageJ (NIH) and Imaris (Bitplane) software. For Olig2 and PLP cell counts in the corpus callosum and spinal cord three animals per genotype and three or more non-adjacent sections for each animal were quantified (n=9–12 sections per genotype). For lesion cell counts, at least three animals of each genotype for each time-point were quantified, and for each animal three or more non-adjacent lesion sections were quantified (n=9–12 sections per genotype). The area of demyelination was measured by staining adjacent sections with solochrome cyanide. All data are presented as mean±standard deviation (s.d.) Comparisons of means between *Olig2-cre*, $Pten^{fl/fl}$ and $Pten^{fl/fl}$ animals was performed using an unpaired t-test. Statistical significance was set at $p<0.01$.

Results

Activation of the PI-3K/Akt/mTOR pathway in *Olig2-cre*, $Pten^{fl/fl}$ spinal cord and cultured *PTEN*-null oligodendrocyte progenitors

In order to investigate *Pten* function in oligodendrocytes and their precursors, we generated conditional $Pten^{fl/fl}$ mice using *Olig2-cre*, which fate maps to all oligodendrocytes[16]. We

first confirmed that *Pten* deletion was efficient and the Pten-regulated pathways were altered in *Olig2-cre, Pten*$^{fl/fl}$ transgenic mice. We observed reduced Pten protein levels, increased levels of phosphorylated Akt (Thr308 and Ser473), and increased levels of phosphorylated p70 S6 Kinase (Thr389) in six month-old whole spinal cord lysates (Fig 1B). Staining for phosphorylated S6 ribosomal protein (Ser235/236) in the spinal cord of *Olig2-cre, Pten*$^{fl/fl}$ mice revealed enhanced expression of phospho-S6 in oligodendrocytes (Fig 1C), indicating activation of the PI-3K/Akt/mTOR pathway. In cultured oligodendrocyte progenitors (OLPs) we observed dramatically reduced Pten expression in *Olig2-cre, Pten*$^{fl/fl}$ oligodendrocytes compared to control *Pten*$^{fl/fl}$ oligodendrocytes (Fig 1D). Phosphorylated S6 is expressed in some control (*Pten*$^{fl/fl}$) oligodendrocyte progenitors (OLPs), however both the level of expression and numbers of phospho-S6-positive OLPs were markedly increased in *Olig2-cre, Pten*$^{fl/fl}$ OLPs (Fig 1D). Oligodendrocytes in *Olig2-cre, Pten*$^{fl/fl}$ lysolecithin lesions also expressed phosphorylated S6 (Fig 1E) indicating activation of the PI-3K/Akt/mTOR pathway in mutant oligodendrocytes during remyelination. Together, these data confirm the expected deletion of *Pten* and activation of Pten-regulated pathways in oligodendrocytes in *Olig2-cre, Pten*$^{fl/fl}$ mice.

Oligodendrocyte hypermyelination in *Olig2-cre, Pten*$^{fl/fl}$ mice

Forced expression of active Akt causes hypermyelination[13] but this could be due to supra-physiologic expression levels from the transgene. We observed enlarged white matter tracts in the brain and spinal cord of *Olig2-cre, Pten*$^{fl/fl}$ mice that stain intensely for the myelin stain solochrome cyanide (Fig 2A). *Olig2-cre, Pten*$^{fl/fl}$ mice also exhibited macrocephaly and increasing brain weights (Fig 2B) and enlarged spinal cords. Electron microscopy of corpus callosum and ventrolateral spinal cord white matter revealed increased myelin sheath thickness and decreased g-ratios in *Olig2-cre, Pten*$^{fl/fl}$ mice (Fig 2C,D). In the corpus callosum large diameter axons had the greatest reduction in g-ratios. Comparable reductions in g-ratios were found across all axon diameters in the ventrolateral spinal cord (Fig 2D). Similar to results of Flores et al. 2008[13], we found the hypermyelination in *Olig2Cre Pten*$^{fl/fl}$ mice was due to increased myelin production by oligodendrocytes, rather than an increase in oligodendrocyte number or differentiation (Fig 3A–D).

Reduced proliferation and density of OLPs in *Olig2-cre, Pten*$^{fl/fl}$ during remyelination

Lysolecithin injection into the spinal cord white matter is a commonly used model of CNS demyelination with a predictable time-course of remyelination and an inflammatory response that is the consequence of myelin damage rather than the cause of demyelination, as is the case in experimental autoimmune encephalomyelitis (EAE). Together, these features make it suitable for studying the kinetics of remyelination[18]. After focal injection of lysolecithin into white matter demyelination occurs rapidly. OLPs repopulate the lesion between 3–5 days post-injection (dpi), and begin to differentiate into mature oligodendrocytes capable of forming of new myelin sheaths at 10dpi. Remyelination is complete by 14–21dpi.

To establish whether *Pten* function in oligodendrocytes is essential for regulation of remyelination, we injected lysolecithin into the ventrolateral spinal cord of *Olig2-cre, Pten*$^{fl/fl}$ and *Pten*$^{fl/fl}$ controls. Animals were sacrificed at 5, 10, and 14dpi. Lesions were stained for immature (Nkx2.2) and mature (CC1, PLP) and pan-oligodendrocyte (Olig2) lineage markers. We have previously characterized Nkx2.2 as a reliable marker for oligodendrocyte progenitors in the setting of remyelination[17,19, 20]. Consistent with these findings, Nkx2.2 expression in this study peaked at 5 dpi associated with OLP recruitment in lesions, and co-localized with other OLP markers (Olig2, PDGFRα and NG2) but not the mature OL marker PLP.

In order to judge whether OLP differentiated might be accelerated in mutant lesions we assessed the ratio of immature versus mature oligodendrocytes as an index of Nkx2.2+ Olig2+ double-positive cells or PLP+ Olig2+ double-positive cells divided by total Olig2+ cells, respectively. As shown (Fig. 4A, B), there was no significant difference in the percentage of immature Nkx2.2+ cells at all time-points (Fig 4A,B). At 5, 10 and 14dpi the number of mature PLP+ (Fig. 4A, B) and CC1+ (data not shown) cells was not significantly increased between *Olig2-cre, Pten*$^{fl/fl}$ and *Pten*$^{fl/fl}$ lesions. These data indicate that differentiation of *Pten*-null OLPs in a remyelinating setting is not detectably accelerated.

Interestingly, we found that the number of oligodendrocytes was significantly reduced in *Olig2-cre, Pten*$^{fl/fl}$ lesions at all time points (Fig 4C). To determine if this reduction in oligodendrocytes could be due to a reduction in proliferation or increase in apoptosis of *Pten*-null OLPs we performed double labeling for Nkx2.2 and proliferation marker Ki67 or apoptotic marker cleaved Caspase-3 at 5dpi. We observed a significant reduction the percentage of proliferating OLPs (Ki67+Nkx2.2+ cells) in mutant lesions (Fig 4D,E). Apoptotic OLPs (Caspase-3+Nkx2.2+) were not significantly different between *Olig2-cre, Pten*$^{fl/fl}$ lesions and *Pten*$^{fl/fl}$ lesions (*Olig2-cre, Pten*$^{fl/fl}$, 0.02%±0.04; *Pten*$^{fl/fl}$, 0.01%±0.01; $p>0.5$).

Because the innate immune response to demyelination has been shown to be an important trigger for OLP activation[21], recruitment[22–23] and differentiation[24] we stained tissue from lesioned *Olig2-cre, Pten*$^{fl/fl}$ mice for macrophage marker Iba1, T-cell marker CD3, and astrocyte marker GFAP. We found no difference in macrophages, microglia, reactive astrocytes or T-cells between mutant and control lesions at all time-points studied (Fig 4F). We also observed no difference in the expression of SMI-32, a marker of non-phosphorylated neurofilaments expressed on damaged axons, between mutant and control lesions (data not shown).

Myelin sheath thickness of remyelinated axons is not increased in *Olig2-cre, Pten*$^{fl/fl}$ mice

One characteristic of remyelination in humans and rodents is that myelin sheath thickness post-repair is significantly reduced compared to unaffected white matter[25]. Given that *Olig2-cre, Pten*$^{fl/fl}$ animals showed dramatic developmental hypermyelination with markedly decreased g-ratios we therefore asked whether myelin thickness in *Olig2-cre, Pten*$^{fl/fl}$ animals might be increased after remyelination compared with controls. We performed electron microscopy and measured g-ratios in 14, 64, and 90dpi in lysolecithin lesions. Contrary to expectation, we found that remyelinating myelin sheath thickness and g-ratios of *Olig2-cre, Pten*$^{fl/fl}$ lesions at 14, 64, and 90dpi were comparable to remyelinated myelin sheath thickness in control lesions (Fig 5A,B; Supplementary Fig 1). These findings indicate that activation of *Pten*-regulated pathways in oligodendrocytes is essential for developmental myelination, but is dispensable for the regulation of myelin thickness during remyelination. Thus, we observed no detectable benefit of activation of PTEN-regulated pathways during remyelination.

Myelin sheath abnormalities and axon damage is observed in older mice lacking *Pten* function in oligodendrocytes

Because *PTEN* deletion is a common oncogenic mutation in human glioma we screened all animals histologically for neoplasia but could find no evidence of tumor formation. However, we did observe progressive neurological symptoms, including ataxia, in older *Olig2-cre, Pten*$^{fl/fl}$ mice suggestive of progressive neuropathy. At 14 weeks of age, toluidine blue staining of ventrolateral spinal cord revealed abnormalities in myelin sheaths of *Olig2-cre, Pten*$^{fl/fl}$ mice (Fig 6A). Electron microscopy of 20 week-old spinal cord white matter confirmed myelin damage including splitting of myelin lamellae which was not observed in

the white matter of control mice (Fig 6B). At one year of age, axonal degeneration was observed in the cervical spinal cord fasciculus gracilis, indicated by strong expression of SMI-32 a marker of non-phosphorylated neurofilaments and dystrophic axons (Fig 6C).

Another measure of abnormal myelination leading to neurological dysfunction involves the organization of the nodes of Ranvier. Sodium channels form characteristic clusters at internodes between myelin segments at defined lengths along the axon. As shown (Fig 6D), 8 week-old *Olig2-cre, Pten*$^{fl/fl}$ mice have normal expression of contactin-associated protein 1 (Caspr) and sodium channels restricted to internodes. By one year of age, however, *Olig2-cre, Pten*$^{fl/fl}$ mice exhibited disorganization of nodes of Ranvier and loss of Caspr and sodium channels in the degenerating fasciculus gracilis (Fig 6D). These findings indicate that *Olig2-cre, Pten*$^{fl/fl}$ have progressive dysmyelination and loss of normal myelin domain structure, signifying abnormal axon function.

Axon damage in fasciculus gracilis is not due to loss of *Pten* function in axons

The fasciculus gracilis is one of the longest projection tracts in the spinal cord and is composed of peripheral dorsal root ganglion cells axons that project to the brainstem. The cervical spinal cord fasiculus gracilis, the most distal end of these projection neurons, has been previously shown to be susceptible to damage as a result of myelin abnormalities[26, 27]. To rule out the possibility that axonal degeneration in *Olig2-cre, Pten*$^{fl/fl}$ was attributable to loss-of-*Pten* function in dorsal root ganglion neurons that project through the fasciculus we performed fate-mapping experiments with *Olig2-cre, Pten*$^{fl/fl}$*, Rosa26YFPfl*$^{fl/fl}$ mice. Although we confirmed expected *Olig2-cre* activity in somatic motor neurons, these do not contribute to the fasiculus gracilis. Indeed, we did not detect YFP reporter expression in any neurons that send ascending fibers through the fasciculus gracilis, specifically dorsal root ganglion neurons and dorsal horn spinal cord neurons (Supplementary Fig 2). These findings rule out a contribution from loss-of-*Pten* function in neurons that project axons through the fasiculus gracilis and indicate that axon degeneration is due to loss-of-*Pten* function in oligodendrocytes and resulting hypermyelination.

Evidence that axonal degeneration in fasciculus gracilis of *Olig2-cre, Pten*$^{fl/fl}$ animals involves APP signaling

Amyloid precursor protein (APP) death receptor-6 (DR6), and Caspase-6 have been recently implicated in a signaling mechanism specific for axonal degeneration. N-terminal APP (N-APP) has been shown to bind to DR6 and p75^{NTR} receptors, which in turn activate neuronal destruction pathways through BAX activation of Caspase-3 in neuronal cell bodies and Caspase-6 in axons[28]. To investigate whether an APP/Caspase-6 mechanism is involved in axonal degeneration in *Olig2-cre, Pten*$^{fl/fl}$ mice we stained cervical cord sections for APP and Caspase-6 expression. As shown (Fig 6E), we observed strong labeling of N-APP and Caspase-6 restricted to the cervical fasciculus gracilis of *Olig2-cre, Pten*$^{fl/fl}$ mice (Fig 6E). These data suggest that axon degeneration of the fasciculus gracilis in *Olig2-cre, Pten*$^{fl/fl}$ mice involves APP signaling.

Discussion

Regulation of myelination is complex, involving appropriate oligodendrocyte responses to differentiate and extend multilaminar sheaths of plasma membrane around axons often in precise relation to their diameter. The mTOR pathway appears to modulate either the myelination capacity of an oligodendrocyte perhaps by increasing protein translation and ribosomal synthesis and/or by modulating signaling involved in oligodendrocyte sensing of axon diameter. It therefore seemed plausible that modulation of the PI-3Kinase-mTOR pathway could provide a means of normalizing myelin sheath thickness of demyelinated

axons to the size of undamaged myelin sheaths, thereby conferring a greater neuroprotective effect in chronic demyelinating diseases such as multiple sclerosis. Here, we established both the developmental consequences and effects on myelin repair in oligodendrocytes that lack *Pten*, a key repressor of the PI-3K/mTOR pathway in the mammalian CNS. In contrast to expectations, we found a number of adverse consequences of this manipulation including loss of myelin and axon integrity.

Pten function in oligodendrocytes is essential for regulation of myelin thickness during development

The established observation that myelin thickness is correlated with axon diameter has implied the presence of sensitive axon-oligodendrocyte signaling mechanisms. While myelin sheath thickness in the peripheral nervous system is regulated by the neuregulin-1 (NRG1) pathway[29–31], myelin sheath thickness may be regulated in a complex fashion by multiple neuregulin isoforms with region-specific roles in the CNS[32–34]. The PI-3K/Akt/mTOR pathway lies downstream of NRG1 signaling and forced expression of constitutively active Akt in oligodendrocytes driven by a PLP promoter results in enlarged white matter tracts in the brain and increased myelin sheath thickness in the optic nerve[13] an effect that is antagonized by the mTOR inhibitor, rapamycin[14]. We demonstrated that early loss of *Pten* and activation of the PI3K/Akt/mTOR pathway in oligodendrocyte progenitors resulted in no change in the total number of oligodendrocytes or the percentage of mature myelinating oligodendrocytes. Developmental loss of *Pten* function also resulted in hypermyelination similar to supra-physiological levels of phosphorylated Akt indicating that the timing of PI3K/Akt/mTOR pathway activation has the same consequences for myelination.

Pten function is largely dispensable during myelin repair

The lysolecithin model of demyelination has a consistent time-course of remyelination making it an ideal model for studying the recruitment of OLPs, their differentiation into mature myelinating oligodendrocytes, and remyelination efficiency. In this study we demonstrated that inactivation of *Pten* in oligodendrocytes did not enhance recruitment or proliferation of OLPs in lesions and had relatively little effect on the time-course of oligodendrocyte differentiation. Although we used *Olig2-cre* heterozygotes to drive *Pten* conditional inactivation, previous work demonstrates that the *Olig2* heterozygous state does not affect myelin repair in the lysolethicin model relative to wild type[35]. We also found reduced numbers of oligodendrocytes in the lesions of *Olig2-cre, Pten$^{fl/fl}$* mice, an effect that could be explained by the finding of reduced proliferation of OLPs and did not appear to be the result of decreased inflammation that could inhibit oligodendrocyte recruitment into lesions[30] or increased apoptosis of OLPs.

Myelin sheath thickness in short and long-term *Olig2-cre, Pten$^{fl/fl}$* lesions neither was restored to levels of hypermyelination found in the contralateral non-lesioned white matter nor increased to levels found in unlesioned white matter of wild-type mice. This result suggests that there are other extrinsic factors present in the lesion environment that inhibit the oligodendrocyte from extending additional myelin sheaths.

Because oligodendrocytes might have heterogeneous properties based on their localization in the CNS and response to different types of injury, we cannot rule out that other CNS remyelination models (e.g., cuprizone) affecting the brain might show a different and more robust remyelination phenotype. Indeed, the finding that short-term remyelination was equivalent in *Olig2-cre, Pten$^{fl/fl}$* lesions compared to control lesions despite a large reduction in the number of oligodendrocytes in mutant lesions suggests that *Pten*-null oligodendrocytes may have the ability to myelinate more axons compared to wild-type

oligodendrocytes. However, based on our observations, the clinical significance of this is unclear in terms of potential benefit.

Pten-regulated signaling is involved in oligodendrocyte-axon interactions important for myelin structural integrity

Prolonged activation of the PI-3K/Akt/mTOR pathway in *Pten*-null oligodendrocytes and resulting hypermyelination clearly has a negative impact on axon integrity. We demonstrated myelin sheath abnormalities as early as four months of age and severe axonal degeneration in the cervical fasciculus gracilis in one year-old *Olig2-cre, Pten*$^{fl/fl}$ mice. Possible causes of axon injury include secretion of toxic factors from *Pten*-null oligodendrocytes, or alternatively, that axon damage is secondary to myelin structural abnormalities. We favor the later possibility because of the progressive and somewhat restricted nature of the axon damage, prominently seen in the fasciculus gracilis. Indeed, the late axonal degeneration phenotype observed in *Olig2-cre, Pten*$^{fl/fl}$ mice is reminiscent of the phenotypes observed in mice with abnormal levels of PLP/DM20 that display specific axonal degeneration in the fasciculus gracilis after 12 months of age[26, 27]. Thus, abnormal myelin structures in these mouse mutants may be the trigger for axonal injury. Ataxia observed in year old *Olig2-cre, Pten*$^{fl/fl}$ mice could be a result of axonal degeneration (such as that in the fasciculus gracilis) or loss of *Pten* function directly in neurons derived from Olig2 progenitors (such as motor neurons[36], cholinergic septal neurons, and GABAergic interneurons[37]). Because of the long duration before onset of ataxia, we favor the former possibility, i.e., that dystrophic myelination over time contributes to axonopathy, rather than disrupted *Pten*-regulated signaling in neurons as such, which would be expected to have an early onset phenotype.

We demonstrated APP/Caspase-6-mediated axonal degeneration in the fasciculus gracilis of *Olig2-cre, Pten*$^{fl/fl}$ mice. APP has been shown to play a crucial role in the pathogenesis of Alzheimer's disease[38]. APP is a transmembrane protein that undergoes enzymatic processing by proteases resulting in the production of various fragments. Cleavage of APP by α-secretases and β-secretases results in the generation of a soluble N-terminal fragment (N-APP) and a membrane-bound C-terminal fragment. γ-secretases subsequently cleave C-terminal APP generating non-amyloidogenic and amyloidogenic Aβ peptides. Whether hypermyelination, an alteration in the signaling pathways upstream of APP, or a combination of both could trigger an increase in N-APP and activation of Caspase-6 in axons warrants further investigation. *Bace1*$^{-/-}$ mice that have loss-of-function of β-secretase *Bace1* have decreased levels of phosphorylated Akt[32] suggesting an interaction between the Akt pathway and β-secretase. Activation of the PI-3K/Akt pathway in oligodendrocytes could increase expression of β-secretase in oligodendrocytes, increasing cleavage of APP and triggering APP/Caspase-6 mediated axonal degeneration in long axonal tracts.

Evidence suggesting lack of clinical benefit of Pten inhibitors and mTOR agonists on myelin repair and axon integrity

Recent reports have shown improved axonal regeneration after optic nerve crush injury by inhibition of Pten or inhibition of tuberous sclerosis protein 1 (TSC1), a negative regulator of mTOR[39]. However these studies showing enhanced axonal regeneration may be the result of *Pten* loss-of-function in axons since intravitreal injection of Cre adenovirus was used which could cause recombination in multiple cells types including neurons and glia.

Therapies aimed at promoting axon regeneration or myelin repair in MS are by definition chronic in nature given the long time course for biological recovery or ongoing damage of autoimmune damage. Here, we show that chronic activation of the PI-3K/Akt/mTOR pathway in CNS oligodendrocytes can have negative consequences for axonal integrity. We

detected no benefit of *Pten* loss-of-function in oligodendrocytes during remyelination. Our findings do not rule out potential beneficial effects of *Pten* loss in rodent models of ongoing demyelination, such as the EAE model. However, *Pten* loss-of-function in T-cells has been shown to increase inflammation and exacerbate disease course in EAE[40], which is a significant concern for proposed systemic therapies aimed at inactivation of *Pten* or activation of its downstream pathways in MS patients. With no apparent benefit to activation of the PI-3K/Akt pathway in oligodendrocytes in a demyelinating repair setting, resulting myelination sheath abnormalities and axonal degeneration, and possible enhanced tumorigenic potential- therapeutic modulation of the PI-3K/Akt/mTOR pathway would need to be approached with caution, and long-term therapy required for chronic diseases such as multiple sclerosis or pediatric conditions would most likely have negative consequences for myelination and axonal integrity.

Supplementary Material

Refer to Web version on PubMed Central for supplementary material.

Acknowledgments

This work was supported by grants from the National Multiple Sclerosis Society (to RJMF and DHR), the United Kingdom Multiple Sclerosis Society (to RJMF), the National Institute of Health (to DHR), and the Medical Scientist Training Program at the University of California, San Francisco (to EPH). DHR is a Howard Hughes Medical Institute Investigator.

References

1. Nave KA, Trapp BD. Axon-glial signaling and the glial support of axon function. Annu Rev Neurosci. 2008; 31:535–561. [PubMed: 18558866]
2. Billiards SS, et al. Myelin abnormalities without oligodendrocyte loss in periventricular leukomalacia. Brain Pathol. 2008; 18:153–163. [PubMed: 18177464]
3. Carson KR, et al. Monoclonal antibody-associated progressive multifocal leucoencephalopathy in patients treated with rituximab, natalizumab, and efalizumab: a Review from the Research on Adverse Drug Events and Reports (RADAR) Project. Lancet Oncol. 2009; 10:816–824. [PubMed: 19647202]
4. Patrikios P, et al. Remyelination is extensive in a subset of multiple sclerosis patients. Brain. 2006; 129:3165–3172. [PubMed: 16921173]
5. Smith EJ, Blakemore WF, McDonald WI. Central remyelination restores secure conduction. Nature. 1979; 280:395–396. [PubMed: 460414]
6. Irvine KA, Blakemore WF. Remyelination protects axons from demyelination-associated axon degeneration. Brain. 2008; 131:1464–1477. [PubMed: 18490361]
7. De Stefano N, et al. Axonal damage correlates with disability in patients with relapsing-remitting multiple sclerosis. Results of a longitudinal magnetic resonance spectroscopy study. Brain. 1998; 121(Pt 8):1469–1477. [PubMed: 9712009]
8. Trapp BD, Nave KA. Multiple sclerosis: an immune or neurodegenerative disorder? Annu Rev Neurosci. 2008; 31:247–269. [PubMed: 18558855]
9. Shields SA, Gilson JM, Blakemore WF, Franklin RJM. Remyelination occurs as extensively but more slowly in old rats compared to young rats following gliotoxin-induced CNS demyelination. Glia. 1999; 28:77–83. [PubMed: 10498825]
10. Rist JM, Franklin RJM. Taking ageing into account in remyelination-based therapies for multiple sclerosis. J Neurol Sci. 2008; 274:64–67. [PubMed: 18539300]
11. Irvine KA, Blakemore WF. Age increases axon loss associated with primary demyelination in cuprizone-induced demyelination in C57BL/6 mice. J Neuroimmunol. 2006; 175:69–76. [PubMed: 16626812]

12. Franklin RJM, Ffrench-Constant C. Remyelination in the CNS: from biology to therapy. Nat Rev Neurosci. 2008; 9:839–855. [PubMed: 18931697]
13. Flores AI, et al. Constitutively active Akt induces enhanced myelination in the CNS. J Neurosci. 2008; 28:7174–7183. [PubMed: 18614687]
14. Narayanan SP, Flores AI, Wang F, Macklin WB. Akt signals through the mammalian target of rapamycin pathway to regulate CNS myelination. J Neurosci. 2009; 29:6860–6870. [PubMed: 19474313]
15. Tyler WA, et al. Activation of the mammalian target of rapamycin (mTOR) is essential for oligodendrocyte differentiation. J Neurosci. 2009; 29:6367–6378. [PubMed: 19439614]
16. Schuller U, et al. Acquisition of granule neuron precursor identity is a critical determinant of progenitor cell competence to form Shh-induced medulloblastoma. Cancer Cell. 2008; 14:123–134. [PubMed: 18691547]
17. Arnett HA, et al. bHLH transcription factor Olig1 is required to repair demyelinated lesions in the CNS. Science. 2004; 306:2111–2115. [PubMed: 15604411]
18. Blakemore WF, Franklin RJM. Remyelination in experimental models of toxin-induced demyelination. Curr Top Microbiol Immunol. 2008; 318:193–212. [PubMed: 18219819]
19. Fancy SP, Zhao C, Franklin RJM. Increased expression of Nkx2.2 and Olig2 identifies reactive oligodendrocyte progenitor cells responding to demyelination in the adult CNS. Mol Cell Neurosci. 2004; 27:247–254. [PubMed: 15519240]
20. Fancy SP, et al. Dysregulation of the Wnt pathway inhibits timely myelination and remyelination in the mammalian CNS. Genes Dev. 2009; 23:1571–1585. [PubMed: 19515974]
21. Glezer I, Lapointe A, Rivest S. Innate immunity triggers oligodendrocyte progenitor reactivity and confines damages to brain injuries. FASEB J. 2006; 20:750–752. [PubMed: 16464958]
22. Arnett HA, et al. TNF alpha promotes proliferation of oligodendrocyte progenitors and remyelination. Nat Neurosci. 2001; 4:1116–1122. [PubMed: 11600888]
23. Kotter MR, Zhao C, van Rooijen N, Franklin RJM. Macrophage-depletion induced impairment of experimental CNS remyelination is associated with a reduced oligodendrocyte progenitor cell response and altered growth factor expression. Neurobiol Dis. 2005; 18:166–175. [PubMed: 15649707]
24. Kotter MR, Li WW, Zhao C, Franklin RJM. Myelin impairs CNS remyelination by inhibiting oligodendrocyte precursor cell differentiation. J Neurosci. 2006; 26:328–332. [PubMed: 16399703]
25. Blakemore WF. Pattern of remyelination in the CNS. Nature. 1974; 249:577–578. [PubMed: 4834082]
26. Anderson TJ, et al. Late-onset neurodegeneration in mice with increased dosage of the proteolipid protein gene. J Comp Neurol. 1998; 394:506–519. [PubMed: 9590558]
27. Edgar JM, et al. Age-related axonal and myelin changes in the rumpshaker mutation of the Plp gene. Acta Neuropathol. 2004; 107:331–335. [PubMed: 14745569]
28. Nikolaev A, McLaughlin T, O'Leary DD, Tessier-Lavigne M. APP binds DR6 to trigger axon pruning and neuron death via distinct caspases. Nature. 2009; 457:981–989. [PubMed: 19225519]
29. Garratt AN, Voiculescu O, Topilko P, Charnay P, Birchmeier C. A dual role of erbB2 in myelination and in expansion of the schwann cell precursor pool. J Cell Biol. 2000; 148:1035–1046. [PubMed: 10704452]
30. Michailov GV, et al. Axonal neuregulin-1 regulates myelin sheath thickness. Science. 2004; 304:700–703. [PubMed: 15044753]
31. Taveggia C, et al. Neuregulin-1 type III determines the ensheathment fate of axons. Neuron. 2005; 47:681–694. [PubMed: 16129398]
32. Hu X, et al. Bace1 modulates myelination in the central and peripheral nervous system. Nat Neurosci. 2006; 9:1520–1525. [PubMed: 17099708]
33. Taveggia C, et al. Type III neuregulin-1 promotes oligodendrocyte myelination. Glia. 2008; 56:284–293. [PubMed: 18080294]
34. Brinkmann BG, et al. Neuregulin-1/ErbB signaling serves distinct functions in myelination of the peripheral and central nervous system. Neuron. 2008; 59:581–595. [PubMed: 18760695]

35. Kotter MR, Setzu A, Sim FJ, Van Rooijen N, Franklin RJM. Macrophage depletion impairs oligodendrocyte remyelination following lysolecithin-induced demyelination. Glia. 2001; 35:204–212. [PubMed: 11494411]

36. Lu QR, et al. Common developmental requirement for Olig function indicates a motor neuron/oligodendrocyte connection. Cell. 2002; 109:75–86. [PubMed: 11955448]

37. Furusho M, et al. Involvement of the Olig2 transcription factor in cholinergic neuron development of the basal forebrain. Dev Biol. 2006; 293:348–357. [PubMed: 16537079]

38. Hardy J, Selkoe DJ. The amyloid hypothesis of Alzheimer's disease: progress and problems on the road to therapeutics. Science. 2002; 297:353–356. [PubMed: 12130773]

39. Park KK, et al. Promoting axon regeneration in the adult CNS by modulation of the PTEN/mTOR pathway. Science. 2008; 322:963–966. [PubMed: 18988856]

40. Johnson TA, Tsutsui S, Jirik FR. Antigen-induced Pten gene deletion in T cells exacerbates neuropathology in experimental autoimmune encephalomyelitis. Am J Pathol. 2008; 172:980–992. [PubMed: 18349128]

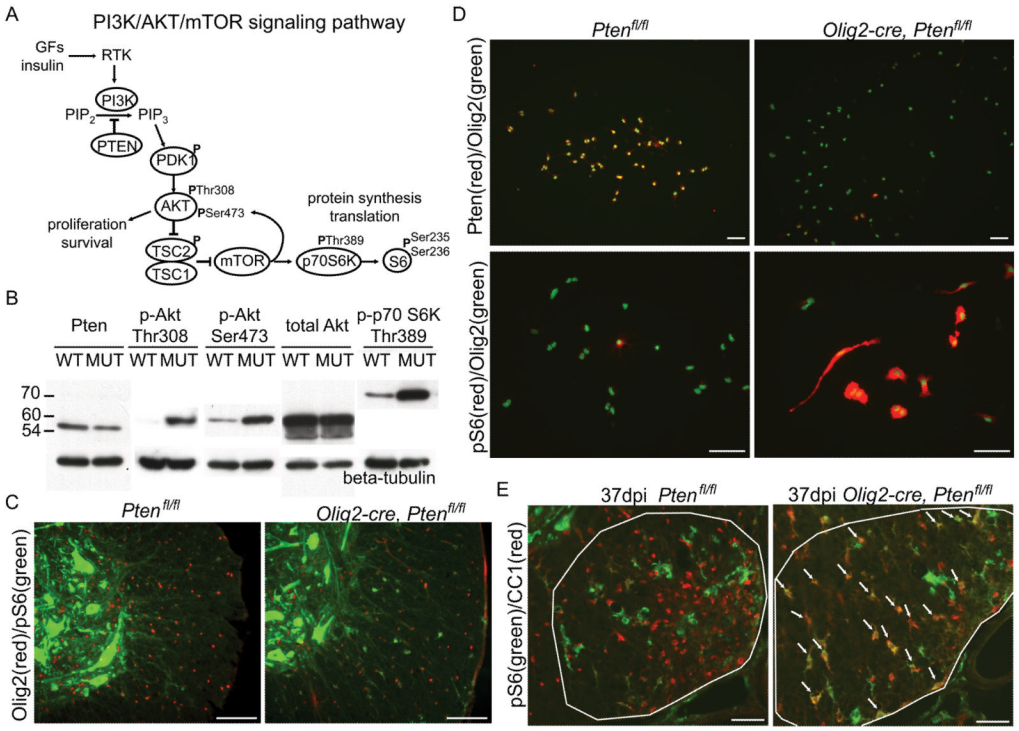

Figure 1.

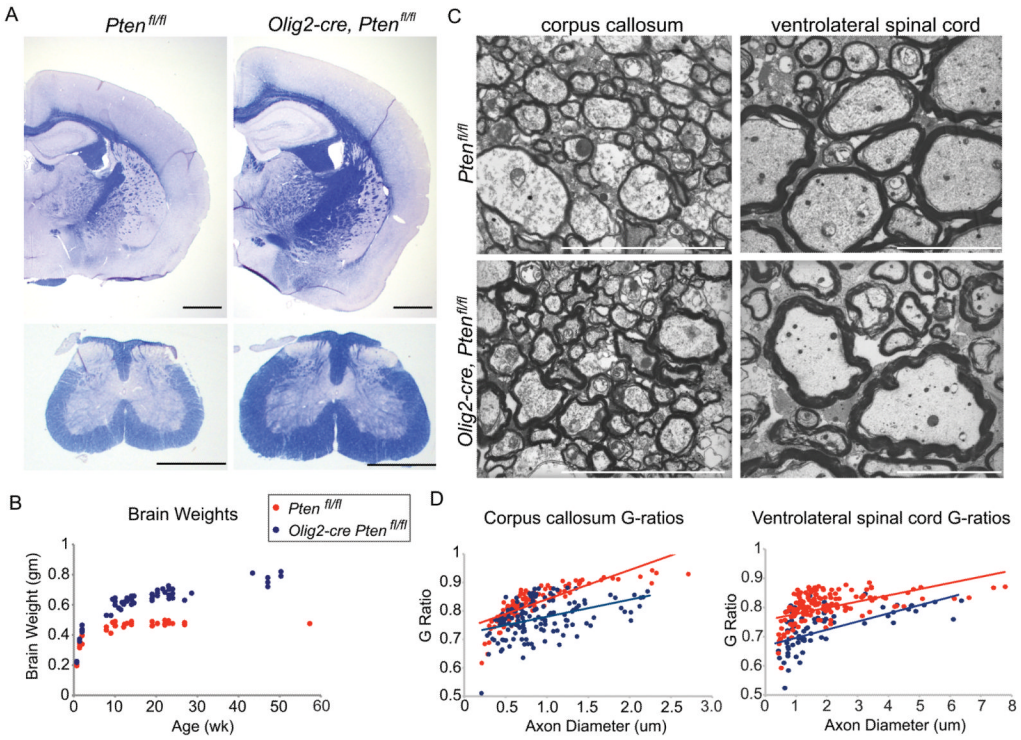

Figure 2.

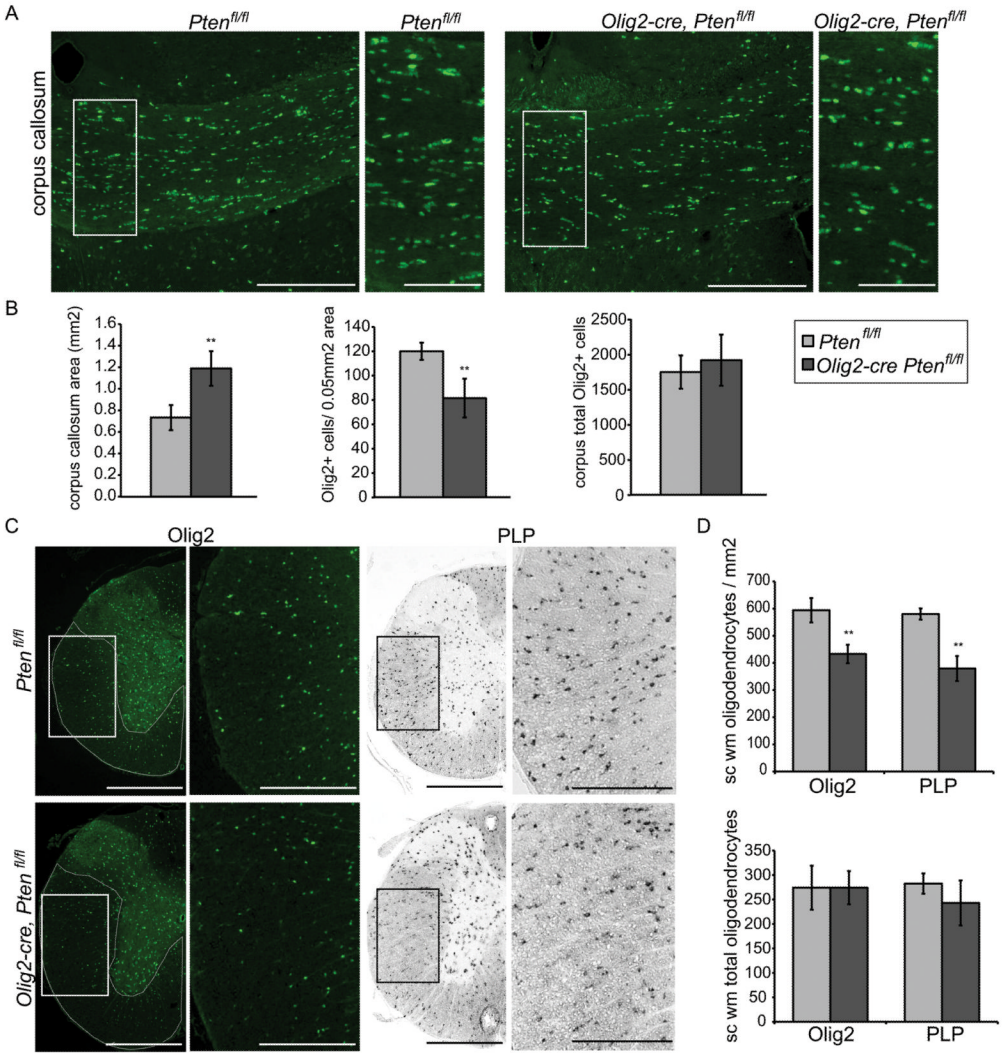

Figure 3.

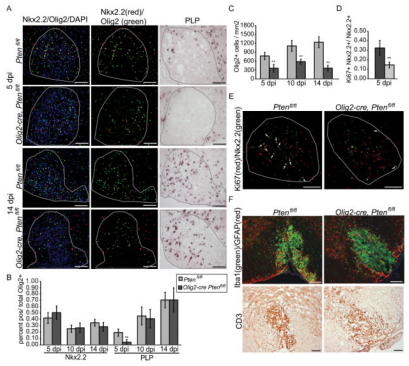

Figure 4.

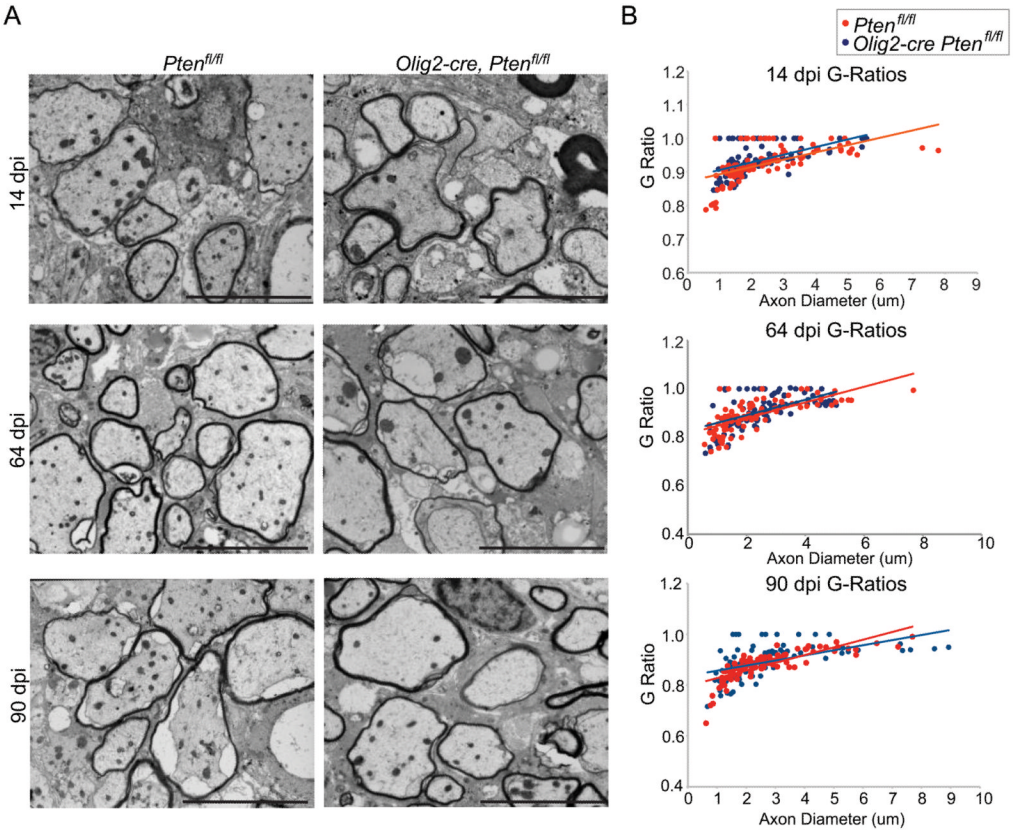

Figure 5.

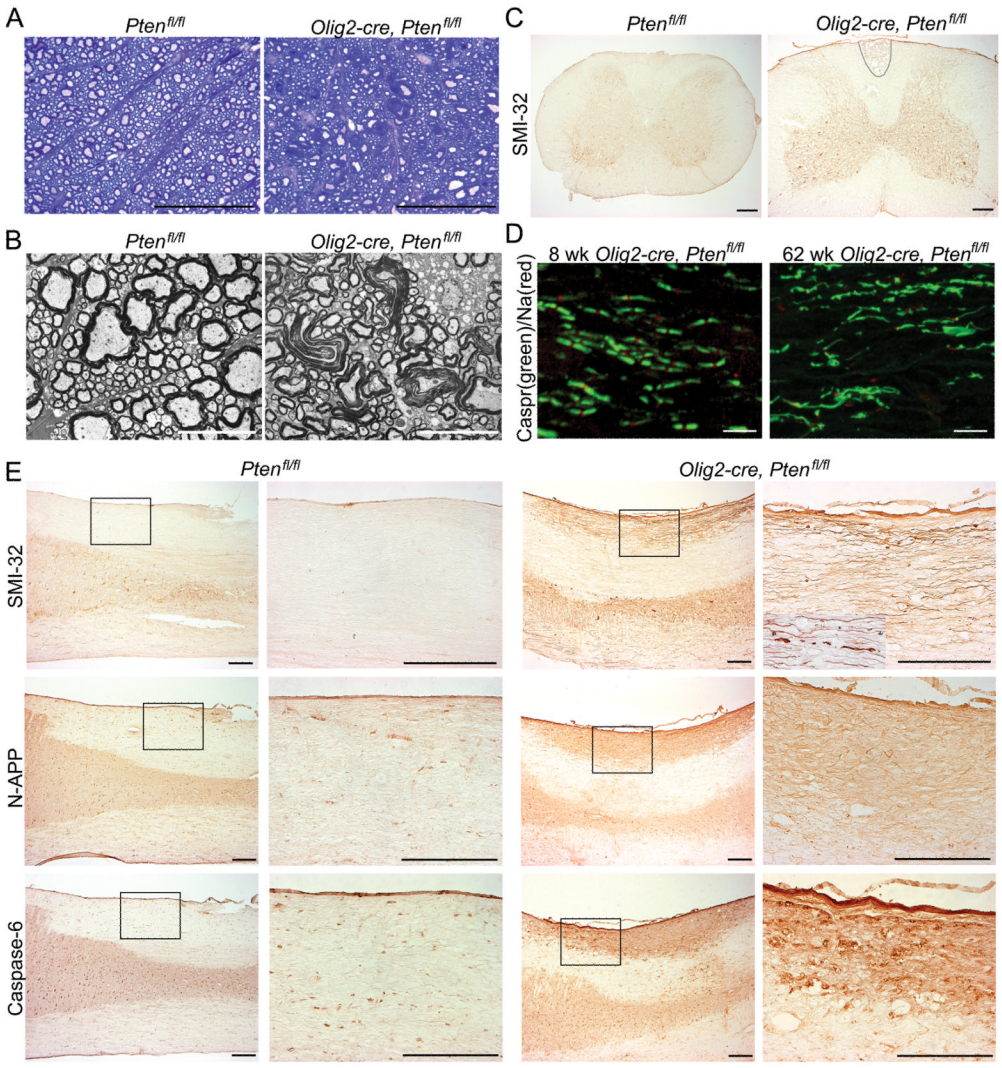

Figure 6.